Title:

The ultrasound guide: katydid ear pinnae code for bat call detection

Running title:

Tympanal pinnae in katydids

Christian Pulver[1], Emine Celiker[1], Charlie Woodrow[1], Inga Geipel[2,3,4], Carl Soulsbury[1], Darron A. Cullen[1], Daniel Veitch[1] & Fernando Montealegre-Z[1,5]

[1]University of Lincoln, School of Life Sciences, Joseph Banks Laboratories, Green Lane, Lincoln, UK, LN6 7DL

[2]Smithsonian Tropical Research Institute, Apartado 0843-03092, Balboa, Panama.

[3]CoSys Lab, Faculty of Applied Engineering, University of Antwerp, 2020 Antwerpen, Belgium

[4]Flanders Make Strategic Research Centre, 3920 Lommel, Belgium

[5]Lead contact

*Correspondence: fmontealegrez@lincoln.ac.uk

eceliker@lincoln.ac.uk

Keywords: Orthoptera, bioacoustics, ultrasound hearing, bat predation, cuticular pinnae, pressure – time difference receiver

Abstract

Early predator detection is a key component of the predator-prey arms race, and has driven the evolution of multiple animal hearing systems. Katydids (Insecta) have a sophisticated ear consisting of paired tympana on each foreleg that receive sound externally and internally, creating a pressure-time difference receiver system capable of sensitive and accurate directional hearing, despite the katydid's small size. Some katydid species have pinnae of unknown function, which form cavities around the outer tympanal surfaces and have been hypothesised to influence the external sound paths. Combining experimental biophysics and numerical modelling on 3D ear geometries, we investigated pinna function in the katydid *Copiphora gorgonensis*. Pinnae induced large sound-pressure gains that enhanced sound detection at high ultrasonic frequencies (>60 kHz), matching the echolocation range of their nocturnal insectivorous bat predators. Comparing pinna resonances of sympatric katydid species supported these findings, and suggests that pinnae may have evolved for enhanced predator detection.

Introduction

Throughout the animal kingdom, the need to localize sound signals, both to detect conspecifics and to avoid predation, is a major evolutionary selection pressure. As a result, vastly different species have convergently evolved mechanisms of hearing to fulfil similar functions[1,2], and hearing organs have evolved in closely related taxonomic groups many times independently[3–5]. To effectively determine the location of a sound source, an animal with two ears will utilize interaural time and amplitude differences. Such binaural auditory systems must satisfy three requirements to function: (1) the distance between each ear must be sufficient to produce recognisable differences in sound arrival time, (2) the ears must be

separated by a body which is large enough to attenuate sound between each ear, (3) the ears must be neurologically coupled in order to calculate time and amplitude differences[6,7]. However, small animals such as insects are theoretically too small to exploit diffractive effects of sound on their bodies to perceive minute differences in sound delays and intensities[8]. To increase the interaural distance, insects like katydids (Orthoptera: Tettigoniidae) have evolved independently functioning ears located in their forelegs[9]. Many species have also evolved the ability to produce and detect ultrasonic frequencies[10], meaning that the resulting distance between the ears provides sufficient spatial separation to exceed the shorter wavelengths of incoming conspecific sounds[2]. Similar to the mammalian ear, the tettigoniid ear has an air-filled ear canal (EC), also called acoustic trachea, delivering the sound to the tympana. Further, in the tettigoniid ear the EC amplifies the sound signals[11–18] and reduces propagation velocity[11,12,18] due to its narrowing, exponential horn design. Sound enters the EC through a specialised opening in the prothorax known as the acoustic spiracle[19]. The EC leads the sound through the thorax and the leg to the internal tympanal surface in the ear of the foreleg. In addition, the tettigoniid ear can also receive sound directly at the ear at the external tympanal surface. Thus the tettigoniid ear functions as a pressure – time difference receiver[2,11–18,20] unlike mammalian ears, which functions as a single input pressure receiver via the EC.

At the external auditory input, certain tettigoniids also possess cuticular pinnae (also referred to as folds, flaps or tympanal covers) partially enclosing their tympana (Fig. 1). Early observations made by Autrum[21,22] suggested that the cuticular pinnae aided the insect to determine the direction of sound, effectively acting as a sound guide. The prominence of cuticular pinnae present in a variety of Pseudophyllinae and Conocephalinae species (see examples in the Supplementary Fig. S1) generated more interest in Autrum's observations. Morphologies of cuticular pinnae vary greatly between species, and were first categorized in

a phylogenetic context by Bailey[9]. Bailey and Stephen[23] proposed a dual functioning auditory system in the tettigoniid *Mygalopsis marki* to explain differences in the auditory morphologies in spiracle size and tympanal pinnae in which the external tympanal ports appears to function as omnidirectional receivers and the EC combined with the spiracle operate as a highly sensitive non-directional receiver. An investigation by Stephen and Bailey[24] corroborated those findings in *Hemisaga* sp. where the authors demonstrated increased acoustic sensitivity at the external tympanal port (through blocking the entrances or slits from here forth). The authors concluded that the dual channel system consisting of the EC and spiracle serve for the detection of predators whilst the external tympanal ports are used for detecting conspecific communication signals[24]. Studies of ultrasonic rainforest pseudophyllines provided more evidence of principal sound reception for conspecific communication using the external tympanal port as a consequence of exceptionally small spiracle sizes[25]. It was reported by the authors that diffraction of very short wavelengths along the tympanal slits contributed to directional orientation in rainforest katydids.

Despite these findings, the role of cuticular pinnae has been subject to considerable debate in the literature. Before experimental evidence of the dual port system in katydids was published[11,18], attention was given to the EC as the main port for sound capture[16,26–30]. Moreover, Michelsen and Nocke[27] argued that the size of the ear is considerably smaller than the wavelengths of most carrier frequencies of described insects known at the time, and therefore the sound pressure field around the ear would be constant and yield no directional cues. In other words, sound accessing the external tympanal port is not related to the direction of incidence, and tympanal pinnae are merely protective features sheltering the fragile tympanum. Montealegre-Z and Robert[31] showed that quieter, low amplitude sounds waves acting on the external tympanal membrane (without gain from the EC) of the Neotropical katydid *Copiphora gorgonensis* (Tettigoniidae: Copiphorini) do cause vibrations of

significant amplitude in the inner ear. Therefore, even these very weak vibrations are mechanically transduced. The external sound arrives 60-80 µs before its amplified form of self on the internal tympanal surface via EC, and this significant phase delay forms the basis of the pressure – time difference receiver definition[11,12]. In katydids with cuticular pinnae surrounding the tympana, evidence suggests that the insect can use both ports, but how the external port contributes to directionality remains unknown[32].

Here, we investigate the role of cuticular pinnae using the neotropical katydid *Copiphora gorgonensis*, a species endemic to the Gorgona Natural National Park, an island in the Pacific Ocean off the western coast of Colombia[33]. *Copiphora gorgonensis* has become a model species for hearing studies due to the transparency of the cuticle which facilitates non-invasive, real-time measurements of the inner ear[1,31,33]. We integrated experimental biophysical measurements based on micro – scanning laser Doppler vibrometry (LDV) and micro-computed tomography to simulate the function of the cuticular pinnae and how they contribute to auditory orientation in katydids. The coupling of the modalities was applied to 3-dimensional (3D) print models of the copiphorine ear, and scaled experiments were performed to validate the simulations. We investigated if: (1) the direction of incidence of the sound stimulus, presented by a loudspeaker, is a function of the sound wave directly accessing the tympana through the slits; (2) the tympanal chambers produce sound pressure gains that act externally on the tympana; (3) tuning properties of the pinnal cavities are a result of pinnal geometry and can be predicted by the volume of the cavity and the size of the entrance to the cavity.

Based on Autrum's original observations, we hypothesized that tympanal pinnae function as ultrasonic guides by pinnae forming exceptionally small, but cavernous cavities. Further, we hypothesized that these cavities act as Helmholtz-like resonators able to capture and amplify diminishing ultra-high frequency waves. In contrast to katydids that also possess pinnae but

rely on a single input configuration, the external copiphorine port participates in predator detection.

Results

Time domain response of the external tympanal port

We investigated the role of tympanal pinnae in sound capture by testing how the direction of incidence of the sound stimulus presented by the loudspeaker induced tympanal displacements at three frequencies (23, 40 and 60 kHz) with the cuticular pinnae intact and later ablated. A total of 2,736 measurements were performed on 13 ears (1,512 measurements for male specimens; 1,224 for female specimens). For time to sound arrival, we found a significant interaction between the presence of cuticular pinnae with angle of incidence and with frequency (Supplementary Table S1). Post hoc analysis showed the presence of pinnae significantly slowed the time of arrival at 23 kHz (t-ratio = -11.15, $P < 0.001$) and 40 kHz (t-ratio = -7.43, $P < 0.001$), but not at 60 kHz (t-ratio = -1.86, $P = 0.063$; Fig. 2B). The effect of tympanum on time of arrival and displacement amplitudes was found to be significant (Supplementary Table S1).

For displacement amplitude, we found that there was a significant interaction between the presence of pinnae and frequency (Supplementary Table S1). Post hoc analysis showed greatest displacement amplitudes at 23 kHz with the pinnae ablated (t-ratio = 3.20, $P < 0.001$; Fig. 2C), which demonstrates that pinnae do not enhance auditory perception of the carrier frequency in *C. gorgonensis*, and that the tympanum achieves this displacement by resonance (see[1,11]). There were no differences at either 40 kHz (t-ratio = 0.84, $P = 0.399$) and 60kHz (t-ratio = -0.61, P=0.540). Across all frequencies, there was a sharp decline in displacement amplitudes at 40 kHz (23 vs 40 kHz: t-ratio = 20.55, $P < 0.001$) and 60kHZ (23 vs 40 kHz: t-

ratio = 19.72, $P < 0.001$), but no difference between 40 and 60 kHz (t-ratio = -0.83, $P = 0.687$; Fig. 2C). We also found a significant interaction between the presence of cuticular pinnae with angle of incidence showing the impact of pinnae in increasing arrival time as the sound source rotates opposite the ear (Supplementary Table S1). Responses were strongest for sound presented perpendicular to each respective slit cavity with the area of the cuticular septum bifurcating the cavities, also referred as "point zero," obtaining the lowest displacement amplitudes with the pinnae intact. Contrarily, point zero showed the greatest displacement amplitude with the pinnae ablated with incident angles on either side of point zero showing a gradual subdued response to the stimulus.

Anatomical measurements of the external tympanal port

2D measurements of the slit area, pinnal protrusion area, septum width, and slit dimensions were studied using an Alicona Infinite Focus microscope ($n = 8$). We found that the size of the entrance of the cavity was not significantly different between the ATM and PTM (Wilcoxon paired rank sum test, $P = 0.958$). The distance between the septum and the outer edge of the pinnae showed that the protrusion area of the PTM was significantly larger than the ATM (two sample t test, $t(14) = -4.64$, $P < 0.001$).

The 3D measurements of the tympanal cavity volumes and cross section of the ears showed that the PTM cavity volume was slightly larger than the ATM volume (Wilcoxon paired rank sum test, $P = 0.958$). The mean cross-sectional width of the ear was 1.143 mm ± 0.353 ($n = 8$).

Tympanal cavity resonance calculations

We used the 2D (slit area) and 3D measurements (cavity) to estimate resonance of the tympanal cavities (Supplementary Table S2). This was calculated by the assumption that the slit openings are a perfect circle (to determine radius) and the cavity acts as a cylindrical tube using a neckless Helmholtz resonance equation. Here, c is speed of sound in air (343 m s^{-1}), S is cross-sectional area of the opening with radius r, 1.85 is the correction length of the neck and V denotes the volume of the resonator / cavity[34].

$$f(h) = \frac{c}{2\pi}\sqrt{\frac{1.85r}{V}}$$

The tympanal chambers (n = 8) showed a neckless Helmholtz resonance of 94.280 ± 3.532 kHz for the ATM and 91.694 ± 3.929 kHz for the PTM (Wilcoxon paired rank sum test, P = 0.093).

3D printed model time and frequency domain measurements

The interaction between the presence of pinnae and frequency were found to be significantly affect sound pressure (dB), whilst tympanum did not (Supplementary Table S1). Across all frequencies, the presence of pinnae increased sound pressure, but differences were greatest at higher frequencies (23 kHz: t-ratio = -2.54, P = 0.014; 40 kHz: t-ratio = -8.69, P < 0.001; 60 kHz t-ratio = -15.66, P < 0.001; 110 kHz t-ratio = 41.70, P < 0.001; Fig. 4). More specifically, the greatest pressure gains were detected at 104.65 kHz for both the ATM (24.19 dB) and PTM (27.68 dB) with the pinnae intact. With the pinnae ablated, the greatest pressure gain was found to be 97.98 kHz for both the ATM (8.04 dB) and PTM (7.81 dB).

Numerical results

For sound pressure measurements there was a significant interaction between the presence of pinnae and frequency (Supplementary Table S1). At 23 kHz ears without pinnae had significantly higher sound pressures (t-ratio = 3.45, $P < 0.001$), but the effect was reversed at 40kHZ (t-ratio = -5.94, $P < 0.001$) and 60kHZ (t-ratio = -28.52, $P < 0.001$), with differences increasing as frequency increased (Fig. 2D). There was no effect of angle of sound incidence or tympanum on sound pressures (Supplementary Table S1).

Simulated sound pressure gains (Fig. 3A-C), and their distribution maps (Fig. 3A and 3B) showed the greatest sound pressure gain at a mean value of ~ 118 kHz (ATM mean 121 kHz, PTM mean 115 kHz), and such gains were reduced or lost entirely when the pinnae were removed (Supplementary Table S1; Fig.3D).

Behavioral audiograms

Behavioural audiograms were obtained from nine tethered females walking on a treadmill. Audiograms were obtained with stimuli in the range 20-120 kHz, as this species is entirely ultrasonic (males call with a 23 kHz pure tone). Audiograms show that the startle response of females decline sharply for stimuli between 20 kHz and 35 kHz, however, response remains essentially constant at higher frequencies (Table S3. Fig. S13).

Discussion

To understand the function of cuticular pinnae of katydid ears, we conducted acoustic experiments on living specimens and used micro-CT to produce images for numerical mathematical models and to print 3D print scaled ears. In all our experiments, the pinnae had a significant effect on the sound reception at the tympana. The experimental results of the live specimens show that at 60 kHz, the pinnae significantly enhanced cavity-induced pressure gains. Further, the extent of the pinnal contribution to tympanal displacement amplitude

depends on the incident angle of the sound source at tested frequencies ≤ 60 kHz. The tympanal ear of *C. gorgonensis* naturally resonates at ca 23 kHz, which corresponds to the dominant frequency of the male calling song[33,35]. This was also observed in our experimental results, irrespective of pinnal presence or absence. At ultrasonic frequencies, the pinnae enclosed tympanal membrane of *C. gorgonensis* show stronger mechanical responses due to the resonances of the tympanal cavities. Montealegre-Z and Robert[31] previously demonstrated that even minuscule tympanal displacements in *C. gorgonensis* create large displacement of the *crista acustica* (CA). Tympanal displacements are nearly duplicated in the CA as the effect of the cantilever system with ear response measured though transparent cuticle. Similar findings can be inferred from LDV experiments on *Mecopoda elongata*[36] with an exposed CA. Insect mechanosensory auditory neurons are capable of detecting exquisitely small mechanical displacements, down to 100 pm[37], close to the theoretical limits of sensitivity[38]. Therefore, the sound pressure gain induced by the tympanal pinnae at ultrasonic frequencies (>60 kHz; Fig. 3) should produce sufficient tympanal displacement to create a response in the CA and subsequently electrical response in the auditory receptors.

As a result of the small size of the katydid ear our experiments were limited to testing frequencies in the lower frequency range. Thus we performed numerical simulations to predict pressure amplitudes at frequencies above 60 kHz. In addition, 3D printed ear models were used to experimentally support the simulation results. Our numerical simulations have predicted sound pressure gains in the frequency range of 50 – 150 kHz with mean resonant frequencies of 115 kHz and 121 kHz in the PTM and ATM cavities respectively (Fig. 3C). Between 50 – 60 kHz, detectable pressure gains inside the cavity started to act along the external tympanal membrane with the best gain of about 23 dB found at resonant frequencies. We did not compare the tympanal response between the experimental and numerical data directly, due to the simplifying assumption in the mathematical models that the tympana are

composed of homogeneous material. In reality, the tympanal membrane is composed of materially different layers where the external surface has more chitinous, sclerotized surfaces extending from the tympanal plate to the membrane, while the internal membrane is composed of elastic, tracheal derived material. To test solid boundaries, we 3D printed ears and scaled the sound stimuli to match the ear size. Differences between the numerical and 3D print models results can be attributed to the material properties incorporated for the tympana in the models. When we incorporated the material properties of the 3D ears into the simulations, the resonant frequencies were found to be at ~111 kHz (ATM 112.5 kHz, PTM 109.5 kHz; Supplementary Fig. S2) which is close to the ~105 kHz measured in the 3D print models (Fig. 3E) and ~ 107.5 kHz of the actual cavities themselves (Supplementary Fig. S3). Without the pinnae, pressure gains were dramatically reduced in the simulations. However, a slight resonance was found in both the numerical simulations and 3D print models caused by the incomplete ablation of the pinnal structures (Figs. 3D and 3F).

Ultrasound guides in insects

Other insects with only a single acoustic input system but also with pinnae on their ears, like moths, are endowed with tympanal membranes mechanically tuned to anticipate the high frequencies used by hunting bats[39]. In this scenario, tympanal pinnae could be an evolutionary adaptation for ultrasonic frequency reception similar to the mechanism found in notodontid moths (Notondontidae)[44]. In these moths, cup–like pinnae formed from the abdominal hood are suggested to enhance the reflection of sounds onto the tympanic membrane[44]. With the pinnae ablated, moths entirely lost the ability to localize sounds[40], not only for ultrasonic frequencies.

High frequency singers of the katydid subfamily Pseudophyllinea in general have very small spiracle sizes, long but narrow ECs, and tympana adorned with various forms of cuticular pinnae[41]. Certain pseudophyllines have been shown to depend more on the external sound stimulus for communicating with conspecifics, than for internal sound reception through the EC, if their song carrier frequency is greater than 50 kHz[23–25,42]. Mason *et al*.[25] found that the dominant port for hearing relies on the tympanal slit to spiracle size area ratio where the larger opening dictates principal auditory input. By physically occluding auditory inputs. The authors measured the summed action potentials of the tympanal nerve and found threshold gains in the ultrasonic range in the rainforest katydids *Myopophyllum speciosum* (carrier frequency 81 kHz), *Haenschiella ecuadorica* (carrier frequency 102 kHz) and *Typophyllum* nr *trapeziforme* (carrier frequency 21 kHz) when the spiracle physically occluded. The responses from the hearing system matched their best auditory frequency. This demonstrated the dominance of the tympanal port for sound entry of conspecific frequencies. With the tympanal cavities blocked, *M. speciosum* reported threshold gains of 30 dB SPL (re 20 µPa), *H. ecuadorica* over 50 dB, and *T*. nr *trapeziforme* 20 – 40 dB at their respective best auditory frequencies. Threshold gains above this range were reported with the tympanal chambers occluded showing a possible adaptation to hear predators via the spiracular port. In our study, we avoided physically occluding the acoustic spiracle as the boundary conditions of the EC would change tympanal sensitivity[15,43,44]. Moreover, completely occluding the spiracle would prevent natural venting of metabolic gases (i.e. CO_2) and inhibit equilibration of tracheal gases with atmospheric pressure[12,45]. In *C. gorgonensis*, the spiracle area is large, naturally open on average three times larger than the total area of the tympanal slit (1 mm^2 : 0.3 mm^2) which is inversely related to the scale of pseudophyllines. Nevertheless, reflectance and power transmittance inside the tympanal cavity experience different acoustics dynamics than the EC. Power transmittance of ultrasonic frequencies suffer significant attenuation as a

result of high reflectance of sound waves along the narrowing EC in *C. gorgonensis*[46]. It is unknown how EC morphology in the Pseudophyllinae functions, let alone how it positively affects sound pressure of ultrasonic frequencies for EC conduction if the system does not rely on a single input.

By concentrating or funnelling ultrasonic energy into the tympanal cavity, the pinnae enhance ultrasonic reception of incidental sounds. The cavity induced pressure gains are the consequence of geometry of the tympanal slit in relation to the geometry and volume of the cavity (Supplementary Table S2). High ultrasonic frequencies that are entering directly and diffracting along the slit edges as each pinnal structure of the ear becomes larger than 1:10 the wavelength of the perceived sound[47]. These imparted forces are magnified by the motion of the tympanum. The resonances afforded by the pinnal structures are evident as both the mathematical and 3D print models do not include a vibrating tympanum. In katydids, irrespective of incident sound pressure magnitude, the cavities provide a consistent pressure gain of at least 13 dB within the frequency range 100 – 120 kHz (Fig. 3C). This in contrast to tympanate moths that depend on the incident sound intensity for mechanical tuning high frequency bat calls[39,40,48] to produce gains up to 16 dB[40].

The ATM slit opening is slightly larger than the PTM, but the PTM has a larger cavity. This causes differences in pressure gains and resonances between both sides. In *C. gorgonensis*, the PTM pinnal structure is approximately 13% larger than the ATM. This increases the micro-acoustical diffraction of ultrasonic frequencies entering the PTM chamber and provides the necessary phase delays to locate sounds. Bailey et al.[49] observed similar pinnal asymmetries in the katydid *Oxyecous lesnei* but the ATM structure was much larger than the PTM which suggests that each tympanum is differentially tuned (for other examples see Fig. 1[50]; Supplementary Fig. S4). Here, we showed that the tympanal cavities and their asymmetric openings act as Helmholtz resonators at frequencies of 94.28 kHz for the ATM

and 91.594 kHz for the PTM in *C. gorgonensis*. Though the simulations show a peak of 118 kHz (ATM 121 kHz, PTM 115 kHz), the Helmholtz calculation assumes the slit opening is a circle and the cavity is a solid walled sphere. Pressure distribution maps from the mathematical models suggest that at 110 kHz (see Fig.3A), the resonance of the pinnae may function in a piston motion, whereby fluctuating air movements are present at the opening of each independent cavity: an observation characteristic of Helmholtz resonance. Sound pressure gains inside the 3D printed model tympanal cavities and resonances closely matched the simulated numerical models (Fig. 5), showing a net average sound pressure gain of 16.1 dB for the ATM and 19.87 dB for the PTM at 105 kHz.

The asymmetry of the tympanal cavities have an acoustic function. Our results show that pinnae cause intra-aural time differences and oscillation phase shifts at ultrasonic frequencies between vibrations in the ATM and PTM (Fig. 2A). This contributes to differences of intensity and arrival of sound that induce pressure gains of ultrasonic frequencies (Fig. 3C). Differential intra - aural tympanal mechanical responses have also been found in the pinnae possessing paleotropical katydid *Onomarchus uninotatus* where the ATM exhibits tuning to the conspecific call and the PTM's response is tuned to higher frequencies suggesting a possible mode for predator detection[51]. The ATM of *C. gorgonensis* is tuned to higher frequencies than the PTM, but how this relates to ecology and behaviour remains unknown as both are connected to the same mechanoreceptor cells. Not only do pinnal structures provide a long diffractive edge for sound waves, but the dorso-ventral asymmetry between the ATM and PTM pinnae may function similar to owl ears where pinnal based cues provide exceptional directional information for ultrasonic reception[52]. Owl ears are positioned asymmetrically with one ear lower than the other which causes prey calls to reach the owl's ears at different times. Following the same concept, we argue that it is possible for a single ear to obtain directional cues for sound localization at frequencies emitted by hunting bats

during echolocation with a single ear due to the asymmetries within. Considered that the tettigoniid ear is capable of resolving such small differences in time and intensity[9,49], it could receive the direction of an attacking bat and engender ultrasound - triggered defensive behaviour[53].

In *C. gorgonensis*, the dual inputs of the spiracle and the external port function as a sound pressure gain compensation system. As previously shown for *C. gorgonensis*[46], and in other species[18,41], the spiracular port and the EC with its exponential horn geometry act as a bandpass filter limited in providing pressure gains to high ultrasonic frequencies (>50 kHz)[12,13] and designed to favour the specific carrier frequency. The level of sound entering the spiracle depends on how the incident soundwave accesses the spiracular opening[49]. The effect of the EC geometry in reducing sound velocity is as much as ~20% or ca 60 µs, and coupled with the contralateral EC, collectively a total of eight inputs are possible with each causing a vibration with variable delays in four internal and four external tympanal surfaces to the same stimulus[12]. Though the reduction in velocity contributes exceptional binaural directional cues, the external port provides real-time sensitivity to exploit unamplified, fading ultrasound. Without time delays, the ear pinnae act as extreme ultrasonic guides that resonate at frequencies closer to the call of common bat predators. Hence the EC might be an impractical and even a more dangerous mode to detect attacking bats as the direction of the angle of incidence accompanied by time delays shorten reaction time and obfuscate the localisation of the predator.

Bat detection by resonance

The island of Gorgona is home to over 33 bat species with many remaining undescribed and underrepresented in wildlife inventories, including least three substrate gleaning bats of the

family Phyllostomidae[54]. Neotropical katydids have evolved sophisticated auditory features as strategies for survival against substrate gleaning bats[55–59]. The habitat of *C. gorgonensis* is in the understory vegetation, often dense vegetation of the tropical forest[60]. In this environment, acoustic signals are heavily attenuated which leads to significant transmission loss[61], but insects have evolved sophisticated receivers to perform call discrimination in these acoustically challenging environments[62]. Adaptations by katydids to bat evade predation include the use of narrow bandwidth, high frequency carrier frequencies, and sporadic calling in order to diminish signal proliferation in the acoustic environment[55,63–65], and ergo evade eavesdropping by bats[66]. Certain adaptations are a trade-off as the katydid becomes more conspicuous and vulnerable to small mammals and for katydids that perform vibrotaxis, even tremulations can attract bats[67,68] other predators like spiders[69]. Likewise, bats foraging at this level also face similar acoustic shortcomings, affecting their echolocation abilities[70]. Thus, several phyllostomid substrate gleaning bats are very well adapted to listen to prey-produced sounds like rustling noises or mating calls of, e.g., male katydids[55,71]. However, at least one gleaning bat species, *Micronycteris microtis* (Phyllostomidae), uses a sophisticated echolocation strategy to discriminate the location of katydids concealed in vegetation[72,73]. Despite passive acoustic defences, calling from restrictive locations and equipped with very large mandibles and sharp fastigia, katydids like *C. gorgonensis* are predated by phyllostomid bats[59].

Here we argue that the pinnal structures of the external tympanal ports of katydid ears act as sound guides providing acute ultrasonic hearing allowing the detection of echolocation calls of hunting bats and thus an additional sensory based defence in the predatory-prey arms race. The presented numerical and experimental evidence suggests that the greatest ultrasonic gain of the pinnae is at frequencies matching those falling into the frequency range of the echolocation calls of native bat species (Fig.5). As neotropical bats approach their target, they

emit short, broadband, multi-harmonic sweeps, demodulate the frequency from higher frequencies above 135 kHz to as low 35 kHz[72,74]. In terms of predator detection, a katydid like *C. gorgonensis* has an excellent chance of detecting the calls of a hunting bat even at the start of the sweep. Responses to these high frequencies are supported by behavioural audiograms that show responses to bat call frequencies (Supplementary Table S3, Fig. S3). A gain of 13 – 20 dB at the start of the bat call provides essential awareness time (≤ 0.86 ms in terms of duration of the complete sweep[72]) to *C. gorgonensis* as a result of the tympanal pinnae.

Katydids with tympanal pinnae on their ears may have initially evolved such sophisticated hearing devices to survive nocturnal predators while they sing under the cover of darkness. Sympatric katydids with pinnae and also potentially predated by bats like *C. gorgonensis* exhibit similar cavity induced pressure gains in the range of phyllostomid bats (Supplementary Fig. S5). It is likely that predation pressures in the island of Gorgona have driven the evolution of katydid pinnae to enhance the resonance of bat calls as evidenced by *Supersonus aequoreus* and *Eubliastes aethiops*.

The pressure – time difference receiver of *C. gorgonensis* is a unique system that can capture different ranges of frequencies between the multiple entry ports that can atone the limitations of each but is also capable of compensating for limitations in auditory orientation[12]. For katydids, incident sounds from elevation are difficult to perceive[32]. The ability of the external port to be positioned and rotated in accordance with the movement of the foretibial knee and foretibial leg joints permits for the ear to be more vertically oriented. The μ-CT imaging presented here of the tympanal cavities supports the theory for vertical orientation as the sub-slit cavity is asymmetrically recessed to the distal end, which is likely to enhance mechanical responses to vertical stimuli (Fig. 1D). For ultrasonic reception, a total of four asymmetrical external ports may be behaviourally articulated in a manner to enhance the

detection of elevated bat calls, and the physical separation between the external ports of each ear yield sufficient binaural cues.

Katydid ear pinnae and the fossil record

The presence of ear pinnae in katydids is unknown in the fossil record. Katydid ancestors (e.g., Haglidae and Prophalangopsidae from upper Jurassic[75]) and early katydids from the middle Paleogene (Eocene, ~ 55 mya[76,77]) all show naked tympana (without pinnae). The earliest echolocating bats are from the Eocene[78], therefore it is likely that ear pinnae evolved in response to bat predation pressures, and could have appeared independently in various clades of Tettigoniidae, but pinnae in the katydid ears have never been mapped in a phylogeny[79]. Analogous ear adaptations are observed in some Eneopterinae crickets (Tribe Lebinthini), which differ from field crickets in their use of high frequencies for specific communication (12 - 28 kHz). These crickets emerged also in the Eocene[80] and while their ancestors exhibit only one functional tympanum (PTM) the extant forms show two functional asymmetric tympana, with the ATM covered by pinnae[81]. Such adaptation suggests a new paradigm of the dual role of the ears, in detecting conspecific calls and bat echolocation.

Several katydids species (e.g., Phaneropterinae, Mecopodiae) exhibit naked tympana (Supplementary Fig. S1B). While little is known about the ecology of many species, some species might have specialised EC designs to increase the range of the bandpass filter[16,18,41] or exhibit behavioural/ecological adaptations that help them to detect or avoid bats. For example, some species might be active during the daytime[82,83], or dwell in dense vegetation that challenges flying[82].

While the diversity of form and function of pinnae in katydids requires a deeper comparative analysis, the presented findings suggest that in the assessed species, pinnae act as ultrasonic

resonators for the early detection of echolocating bats. Given the broad global distribution of echolocating bats and the diversity of their feeding habits, it would be expected that similar adaptations exist in other prey taxa.

Materials and methods

Specimens

Copiphora gorgonensis (Tettigoniidae: Copiphorini) is endemic to Gorgona National Natural Park, Colombia (02°58′03″N 78°10′49″W). The original generation of the species were imported to the UK under the research permit granted by the Colombian Authority (DTS0-G-090 14/08/2014) in 2015. The specimens were ninth generation, captive bred colonies and maintained at 25°C, 70% RH, light: day 11 h: 23 h. They were fed *ad libitum* diet of bee pollen (Sevenhills, Wakefield, UK), fresh apple, dog food (Pedigree Schmackos, UK) and had access to water. Live experiments were conducted on seven adults of *C. gorgonensis* from our laboratory breeding colonies at the University of Lincoln (Lincoln, UK). Following experimentation, these specimens plus an additional four females already stored in ethanol were micro-CT scanned for finite element modelling; totalling 17 ears (10 female, 7 male). Live specimens were preserved in ethanol-filled jars and stored in a freezer at – 22°C at the University of Lincoln (Lincoln, UK).

Vibration measurements

Insects were chemically anesthetized using triethylamine-based agent FlyNap (Carolina Biological Supply, USA) for 15 min prior to the mounting process, and remained awake throughout the duration of the experiment. The animals were dorsally mounted using a

specialized platform to isolate the external and internal sound inputs and also mimic their natural stance. A rosin-beeswax mix was used to fix the pronotum, and the mid and hind legs, to the mount. This specialized platform[11] consists of a two Perspex panels (1.61 mm diameter) that are joined by latex and suspended in the air by a 12 x 12 mm metal frame attached to a micromanipulator (World Precision Instruments, Inc., USA) (see[1]). At the Perspex junction, the forelegs of the insect were extended through arm holes cut in the Perspex and attached on a rubber block with metal clasps. A metal clasp was placed on each foretibia and forefemur (total of 4) to arrest foreleg motion. The arm holes and frame borders were sealed with latex to deny sound propagation to the spiracle.

The LDV system consisted of a the OFV-2520 Dual Channel Vibrometer - range velocity controller for operating two single point laser sensor heads, sensor heads hereafter (OFV-534, Polytec, Germany) each with VIB-A – 534 CAP camera video feed and laser filters. Each sensor head was mounted on a two - axis pivoting stage (XYZ, Thorlabs Inc., USA) anchored to an articulating platform (AP180, Thorlabs Inc., USA) and manually focused at 10.5 cm above a vibration isolation table (Pneumatic Vibration Isolation Table with a B120150B - Nexus Breadboard, 1200 mm x 1500 mm x 110 mm, M6 x 1.0 Mounting Holes, Thorlabs Inc., USA) supported by an anti-vibration frame (PFA52507 - 800 mm Active Isolation Frame 900 mm x 1200 mm, Thorlabs Inc., USA) in an anechoically isolated chamber (AC Acoustics, Series 120a, internal dimensions of 2.8 m x 2.7 m x 2 71 m). The sensor heads were outfitted with magnification microscopic lenses (Mitutoyo M Plan 10x objective for Polytec PSV-500 single laser head OFV 534, Japan) and positioned about 35 to 40 mm away from the insect foreleg at 45° angles towards the Perspex surface (Supplementary Fig. S6). The narrow entrance to the tympanal chambers restricted the use of LDV to measure tympanal responses across the entire tympanal membrane. Therefore, the placement of the sensor heads was limited to positions where the sensor heads were perpendicular to the

tympanic membrane of interest. The sensor speeds were maintained at 0.005 (m/s)/V and recorded using an OFV-2520 internal data acquisition board (PCI-4451; National Instruments, USA).

Tympanal vibrations were induced by a four-cycle sinusoidal wave at 23, 40 and 60 kHz. The closed-field configuration of the loudspeaker restricts the delivery of high ultrasonic stimuli to 60 kHz. A rotating automated stage (PRM1Z8 rotation mount, Thorlabs Inc., USA) with a KDC101 K-Cube™ DC Servo Motor Controller (Thorlabs Inc., USA) positioned a multi-field magnetic loudspeaker (MF1, Tucker Davis, USA) with a parabolic nozzle (see Supplementary Materials from[12]) and plastic probe tip (3.5 cm L x internal diameter 1.8 mm W) about 3.5 mm away from the mounted insect and 10.2cm above the breadboard table. The speaker was moved across a 12 cm semi-circle in 1° steps (0.56 mm). The probe tip was positioned at "point zero" and 20 single shot recordings at 1°, totalling 10° at either side of this port (Supplementary Fig. S7). A high quality 500 band pass filter was applied at 10 to 30 kHz for the 23 kHz recordings, 30 to 50 kHz for the 40 kHz recordings, and 50 to 70 kHz for the 60 kHz recordings. All acoustic signals were generated by a waveform generator (SDG 1020, Siglent, China), synchronized with the LDV, amplified (ZB1PS, Tucker Davis, USA) and measured by a 1/8 (3.2 mm) omnidirectional microphone (Type 4138, Brüel & Kjaer, Nærum Denmark) located about 3 mm from tympanum. The microphone, with built in preamplifier (B&K 2670, Brüel & Kjær, Nærum, Denmark), was calibrated using a sound-level calibrator (Type 4237, Brüel & Kjaer, Nærum, Denmark) and set to 316 mV/Pa output via a conditioning amplifier (Nexus 2690-OS1, Brüel & Kjær, Nærum, Denmark). A reference measurement was performed by placing the microphone 3 mm from the probe tip to the loudspeaker before each experiment. Using a micro-manipulator, the microphone was positioned approximately 3 to 3.5 mm from the ear to monitor the acoustic isolation of the anechoic platform.

Experimental procedures

The sensor heads were manually focused on the external tympanal surface using the 2 - axis pivoting stage and manual wheel with the aid of the sensor head camera output displayed on an LED screen. For the time measurements, the point zero was found for each leg and for each test frequency. The point zero was the point where the displacements from the anterior tympanic membrane (ATM) and posterior tympanic membrane (PTM) matched the oscillation phase of the generated 4-cycle sinusoidal waves. This ensured that the vibrations of the tympanic membranes were synchronous relative to the speaker position. Displacement amplitudes from the same cycle order number were measured from each sensor head reference, and approximately 252 data points were measured per ear.

After recording the vibrations for both insect ears, the cuticular pinnae were carefully excised (not to damage the tympanal organs or the fine layer of tissue ventrally connected to the tympanic membranes) using a razor blade. The measurements were repeated for each ear following the same protocol.

Time and displacement measurements were analysed by identifying the second oscillation of the 4-cycle tone generated waves in each PSV software window (PSV 9.4 Presentation software, Polytec, Germany).

Morphological studies of the ear

To produce 3D data for modelling, 17 ears of *C. gorgonensis* were scanned using a SkyScan 1172 X-ray micro-CT scanner (Bruker Corporation, Billerica, MA, USA) with a resolution between 1.3 and 2.9 µm (55 kV source voltage, 180 µA source current, 300 ms exposure and

0.1° rotation steps). As experimental procedures required removal of the cuticular pinnae, eight additional specimens with intact pinnae were scanned. The micro-CT projection images were reconstructed with NRecon (v.1.6.9.18, Bruker Corporation, Billerica, MA, USA) to produce a series of orthogonal slices. The 3D segmentation of the ear, measurements of the ear cross section and width, and volumetric measurements of the cavities formed by the pinnae were performed with the software Amira-Aviso 6.7 (Thermo Fisher Scientific, Waltham, Massachusetts, USA). Micro-CT stereolithography files (STL) were generated for mathematical modelling using established protocols[11,12] and to 3D print ear models.

For 2D measurements of the cavity slit area, pinnal protrusion, and the distance between the pinnal cavities, an Alicona InfiniteFocus microscope (G5, Bruker Alicona Imaging, Graz, Austria) at x5 objective magnification was used to capture images with a resolution of abou100 nm of collection specimens with pinnae intact (n = 8 ears).

Bat and insect call recordings

The echolocation calls of phyllostomid bats (Chiroptera: Phyllostomidae) native to Gorgona Island were recorded in 2015. The call of *Micronycteris megalotis* was recorded using the Echo Meter Touch 2 (Wildlife Acoustics, Maynard, MA, USA), with a sampling rate of 384 kHz. *Gardnerycteris crenulatum*, *Tonatia saurophila* and *Micronycteris microtis* were recorded in a small indoor flight cage (1.4 x 1.0 x 0.8 m) in which they were allowed to fly via an ultrasound condenser microphone (2 - 200 kHz frequency range, ±3 dB frequency response between 25 - 140 kHz; CM16, CMPA preamplifier unit, Avisoft Bioacoustics, Glienicke, Germany) and real time ultrasound acquisition board (6 dB gain, 500 kHz sampling rate, 16 bit resolution; UltraSoundGate 116Hm, Avisoft Bioacoustics, Glienicke, Germany) connected to a laptop (Think Pad X220, Lenovo, Beijing, China), with a

corresponding recording software (Avisoft RECORDER USGH, Avisoft Bioacoustics, Glienicke, Germany). These are the most common insectivorous gleaning species in the habitat of *C. gorgonensis*. Call description of single calls is presented as Supplementary Fig. S8.

SI Appendix, Section 1 (see Supplementary Fig. S9) has details of male *C. gorgonensis* calling song recording.

Vibrations of synthetic 3D-printed scaled ear models

For time domain measurements, 3D models of the ears were placed on a micromanipulator arm with blu-tac (Bostik Ltd, Stafford, UK) and positioned frontally 30 cm from a MF1 loudspeaker at the same elevation. A 25 mm tipped B&K Type 4182 probe microphone (Brüel & Kjær, Nærum, Denmark) with a 1 × 25 mm (0.99″) probe tube length and 1.24 mm (0.05″) interior diameter, calibrated using a B&K Type 4237 sound pressure calibrator (Brüel &Kjær, Nærum, Denmark) was placed ventral to the ear. The ear moved onto the microphone using an electronic micromanipulator (TR10/MP-245, Sutter Instrument, Novato, California, USA), to a position 1 cm from the back of the cavity. Stimuli delivered were individually scaled to match the wavelength of a real-size ear (e.g., for a 1:10 scale printed model, the frequency delivered to simulate 120 kHz would be 120/10 = 12 kHz) to account for variation in printed model scaling. 3D printed models were scaled 1:11.43 (male 1:11.33; female 1:11.53) with the corresponding average scaled stimuli of 2.01 kHz for 23 kHz, 3.50 kHz for 40 kHz, 5.25 kHz for 60 kHz, and 9.63 kHz for 110 kHz. Four cycle pure tones were produced using a function generator (SDG1000; Siglent Technologies Co. Ltd), and the amplitude set to deliver 1 Pa to the microphone at each frequency. Received signals were amplified using a B&K 1708 conditioning amplifier (Brüel & Kjær, Nærum, Denmark), and

acquired using a PSV-500 internal data acquisition board (Polytec GmbH, Waldbronn, Germany) at a sampling frequency of 512 kHz. The microphone remained stationary during the experiments, nor was its direct path to the speaker obstructed. Instead, the microphone entered the ear via the drilled hole, allowing the pinnae to surround the tip of the microphone. Thus, the reported sound pressure gains result solely from the cavities of the 3D model, and not the motion of the microphone. When the microphone was positioned inside the cavities, the gap between the drilled hole and microphone probe was sealed with blu-tac (Bostik Ltd, Stafford, UK) to mimic the real cavity and avoid acoustic leaking (refer to Supplementary Materials Section 2).

To calculate the frequency that produced the best gain, the MF1 loudspeaker was replaced with a RAAL 140-15D Flatfoil loudspeaker (RAAL, Serbia), with a different amplifier (A-400, Pioneer, Kawasaki, Japan). This speaker was able to deliver a broadband stimulus of periodic chirps, generated within Polytec 9.4 software (Polytec GmbH, Waldbronn, Germany), with a simulated frequency range of 2-150 kHz. Recording in the frequency domain, at a sampling frequency of 512 kHz, the amplitude of the broadband stimulus was mathematically corrected within the software to deliver 60 dB at all frequencies. The reference frequency spectrum with no ear present could be subtracted from the frequency spectrum reported within the cavities to calculate frequency-specific gain and thus cavity resonance. Gain was calculated by subtracting the probe microphone sound pressure (dB) measured 1 cm outside of the cavity from inside the tympanal cavity measurements (Fig. 4; see also Supplementary Materials Section 2).

For comparative purposes, the ears of the following sympatric and pinnae bearing katydid species from the Island of Gorgona were also 3D printed and subjected to experiments according to the aforementioned protocol: *Supersonus aequoreus*, *Eubliastes aethiops*, and Pleminiini sp. (see Supplementary Fig. S4).

Frequency domain recordings of the cavity resonance, and time domain recordings of pure tone gains were then exported as .txt files for analysis. Methods for printing 3D ear models are provided in the Supplementary Materials Section 1.

Mathematical models and numerical simulations

The mathematical models have been constructed as a scattering acoustic – structure interaction problem and simulate the acoustic response of the tympanal cavities to an incident plane acoustic wave in an air domain. Hence, the 3D model considers the interaction of the sound wave with the ear, for which realistic material properties have been incorporated. The air acoustic domain is truncated as a sphere with a 3 mm radius that is centered around the ear (Supplementary Fig. S10). Two different geometries of the ears were taken as part of the mathematical model domain: pinnae intact and pinnae removed (Supplementary Fig. S11).

The models were considered both in the frequency and the time domains, and were solved using the acoustic-shell interaction module of the software Comsol Multiphysics, v5.6[84]. For the frequency domain models, the incident wave was taken to be a chirp with an amplitude of 1 Pa and frequency 2-150 kHz, directed at "point zero" as defined in the in the section *vibrational measurements*. For the time domain models, three different incident waves were used, with amplitudes 1 Pa and frequencies 23, 40, 60 kHz. The direction of the waves was taken as -10°, -5°, 0°, 5° and 10° on a fixed plane perpendicular to the ear, with 0° corresponding to "point zero". The details of the solved system of equations can be found in Supplementary Materials Section 1.

The numerical solution to the problem was obtained using the finite element method for the spatial variables in both the time- and frequency-domain simulations. For forming the finite-element mesh, the maximum diameter used for the tetrahedral elements in the sphere was

$h_{max} = \frac{c}{6 \times f_0}$, where $c = 343\ \mathrm{m/s}$ and $f_0 = 150\ \mathrm{kHz}$ (Supplementary Fig. S10 and S11). Hence, even at the largest frequency considered, there were six tetrahedral elements per wavelength. Quadratic Lagrange elements were applied for the solution.

For the time domain solution, the time variable was solved for using the Generalized alpha method, with a constant time step of $\Delta t = \frac{1}{60 \times 150}$ s, so that the Courant-Friedrichs-Lewy (CFL) condition[85], defined as $CFL = \frac{c \times h_{max}}{\Delta t}$ was 0.1, which gives a reliable approximation of the solution.

Behavioral audiograms

Behavioral audiograms were performed on nine tethered female (*n* = 9) *C. gorgonensis* to test behavioral response thresholds to controlled auditory stimuli (20 – 120 kHz). Methods are provided in Supplementary Materials Section 1.

Statistical analyses

Using empirical data we tested the effect of cuticular pinnae on tympanal responses (in displacement amplitude (natural log transformed) and arrival time) to incident sound, we fitted linear mixed models (LMM) with angle (-10° to 10°, polynomial continuous variable) as a covariate and presence of pinnae (y/n), frequency (23, 40 and 60 kHz, categorical variable), tympanum (ATM or PTM) as fixed factors. We include the interactions between angle and pinnae and between pinnae and frequency. To model the curvature in the response surface of the pinnal enclosed tympanum, angle was fitted as a quadratic polynomial with 0° (at point zero). The interaction of angle and pinnae was fitted as such to show the restriction

of pinnal structures in both time and displacement to the response surface. We carried out post hoc tests between pinnae (y/n) at each frequency using estimated marginal means from the package emmean[86].

To determine differences in both the anatomy and estimated resonance of the anterior and posterior pinnae, we carried out two-sample t-test and Wilcoxon rank sum (or Mann-Whitney U test) depending on data distribution. These anatomical differences included the area of the entrance to the cavity, cavity volume, and protrusion.

Using the same initial LMM model, we tested how sound pressure estimated from numerical models was related to angle (-10° to 10°, polynomial continuous variable), presence of pinnae (y/n), frequency (23, 40 and 60 kHz, categorical variable), tympanum (ATM or PTM) as fixed factors. Again, we include the interactions between angle and pinnae and between pinnae and frequency. We finally tested sound pressure based on 3D models. the presence of pinnae (y/n), frequency (23, 40 and 60 kHz, categorical variable), tympanum (ATM or PTM) as fixed factors, with the inclusion of the interaction between pinnae and frequency. For both numerical and 3D models, we carried out post hoc tests between pinnae (y/n) at each frequency using estimated marginal means from the package emmean.

All LMMs were run using the package lmerTest[87] in R 4.0.0[88]. Statistical tests and graphs were performed on R 4.0.0[88].

Data availability

Experimental data (LDV recordings), numerical simulations, Comsol model files, and µ-CT stereolithography files (in .stl format) are available in Dryad (DOI:).

Acknowledgements

We thank the Orthopterists' Society for aiding in funding the micro-CT work of CW, for which some data has been used in this study, and to the University of Lincoln's School of Life Sciences for CW's PhD studentship.

Author contributions

All authors were involved in writing and revision of the manuscript. CP and FMZ performed acoustic experiments on live specimens. CP and CW designed and performed all 3D print model experiments. CP constructed the speaker mount, automated the controls in the arena, collected and analysed data. CS designed the statistical model and completed statistical analyses. EC developed and performed all numerical models and simulations. CW illustrated figures, conducted µ-CT scans, performed all post-image segmentation for numerical analyses, and conducted 3D printing. IG and FMZ recorded insect and bat acoustic signals. FMZ and CP conceived the idea for the project. FMZ led the lab, assisted with idea development, and provided equipment training.

Competing interests

No competing interests declared

Funding

This research is part of the project "The Insect Cochlea" funded by the European Research Council, Grant ERCCoG-2017-773067 to FM-Z; and was also funded by the Natural Environment Research Council (NERC), grant DEB-1937815 to FM-Z.

References

1. Montealegre-Z, F., Jonsson, T., Robson Brown, K. A., Postles, M. & Robert, D. Convergent evolution between insect and mammalian audition. *Science.* **338**(6109), 968–97 (2012).

2. Robert, D. Directional Hearing in Insects. in *Sound Source Localization* (eds. Popper, A. N. & Fay, R. R.) 6–35 (Springer New York, 2005). doi:10.1007/0-387-28863-5_2.

3. Song, H. *et al.* Phylogenomic analysis sheds light on the evolutionary pathways towards acoustic communication in Orthoptera. *Nat. Commun.* **11**, 4939 (2020).

4. Göpfert, M. C. & Hennig, R. M. Hearing in Insects. *Annu. Rev. Entomol.* **61**, 257–276 (2016).

5. Strauß, J. & Stumpner, A. Selective forces on origin, adaptation and reduction of tympanal ears in insects. *J. Comp. Physiol. A* **201**, 155–169 (2015).

6. Lakes-Harlan, R. & Scherberich, J. Position-dependent hearing in three species of bushcrickets (Tettigoniidae, Orthoptera). *R. Soc. Open Sci.* **2**, 140473 (2015).

7. Suga, N. Principles of auditory information-processing derived from neuroethology. *J. Exp. Biol.* **146**, 277–286 (1989).

8. Hartbauer, M. & Römer, H. From microseconds to seconds and minutes-time computation in insect hearing. *Front. Physiol.* **5 APR**, 1–12 (2014).

9. Bailey, W. J. The ear of the bushcricket. in *The Tettigoniidae. Biology, systematics and evolution* (eds. Bailey, W. J. & Rentz, D.) 217–247 (Crawford House Press, 1990).

10. Strauß, J., Lehmann, A. W. & Lehmann, G. U. C. Sensory evolution of hearing in tettigoniids with differing communication systems. *J. Evol. Biol.* **27**, 200–213 (2014).

11. Jonsson, T., Montealegre-Z, F., Soulsbury, C. D., Robson Brown, K. A. & Robert, D. Auditory mechanics in a bush-cricket: direct evidence of dual sound inputs in the pressure difference receiver. *J. R. Soc. Interface* **13**, 20160560 (2016).

12. Veitch, D. *et al.* A narrow ear canal reduces sound velocity to create additional acoustic inputs in a microscale insect ear. *Proc. Natl. Acad. Sci. U. S. A.* **118**, (2021).

13. Lewis, B. the Physiology of the Tettigoniid Ear. *Methods* 861–869 (1974).

14. Michelsen, A. & Larsen, O. N. Biophysics of the ensiferan ear - I. Tympanal vibrations in bushcrickets (Tettigoniidae) studied with laser vibrometry. *J. Comp. Physiol. A* **123**, 193–203 (1978).

15. Nocke, H. Physical and physiological properties of the tettigoniid (‘grasshopper’) ear. *J. Comp. Physiol. A* **100**, 25–57 (1975).

16. Hoffmann, E. & Jatho, M. The acoustic trachea of Tettigoniids as an exponential horn: Theoretical calculations and bioacoustical measurements. *J. Acoust. Soc. Am.* **98**, 1845–1851 (1995).

17. Larsen, O. N. Mechanical time resolution in some insect ears - II. Impulse sound transmission in acoustic tracheal tubes. *J. Comp. Physiol. A* **143**, 297–304 (1981).

18. Michelsen, A., Rohrseitz, K., Heller, K. G. & Stumpner, A. A new biophysical method to determine the gain of the acoustic trachea in bushcrickets. *J. Comp. Physiol. A* **175**, 145–151 (1994).

19. Kalmring, K. *et al*. The Auditory-Vibratory Sensory System in Bushcrickets (Tettigoniidae, Ensifera, Orthoptera) I Comparison of Morphology, Development and Physiology. in *Environmental Signal Processing and Adaptation* (eds. Heldmaier, G. & Werner, D.) 169–207 (Springer Berlin Heidelberg, 2003). doi:10.1007/978-3-642-56096-5_9.

20. Michelsen, A. & Larsen, O. N. Pressure difference receiving ears. *Bioinspiration and Biomimetics* **3**, 011001 (2008).

21. Autrum, H. Über Lautäusserungen und Schallwahrnehmung bei Arthropoden II. *Z. Vgl. Physiol.* **28**, 326–352 (1940).

22. Autrum, H. Anatomy and physiology of sound receptors in invertebrates. *Acoust. Behav. Anim.* 412–433 (1963).

23. Bailey, W. J. & Stephen, R. O. Directionality and auditory slit function: A theory of hearing in bushcrickets. *Science.* **201**, 633–634 (1978).

24. Stephen, R. O. & Bailey, W. J. Bioacoustics of the ear of the bushcricket *Hemisaga* (Sagenae). *J. Acoust. Soc. Am.* **72**, 13–25 (1982).

25. Mason, A. C., Morris, G. K. & Wall, P. High ultrasonic hearing and tympanal slit function in rainforest katydids. *Naturwissenschaften* **78**, 365–367 (1991).

26. Shen, J. A peripheral mechanism for auditory directionality in the bushcricket *Gampsocleis gratiosa*: Acoustic tracheal system. *J. Acoust. Soc. Am.* **94**, 1211–1217 (1993).

27. Michelsen, A. & Nocke, H. Biophysical Aspects of Sound Communication in Insects. *Adv. In Insect Phys.* **10**, 247–296 (1974).

28. Eisner, N. & Popov, A. V. Neuroethology of Acoustic Communication. in vol. 3683

229–355 (1978).

29. Hill, K. G. & Oldfield, B. P. Auditory function in tettigoniidae (Orthoptera:Ensifera). *J. Comp. Physiol. A* **142**, 169–180 (1981).

30. Yack, J. E. The structure and function of auditory chordotonal organs in insects. *Microsc. Res. Tech.* **63**, 315–337 (2004).

31. Montealegre-Z, F. & Robert, D. Biomechanics of hearing in katydids. *J. Comp. Physiol. A Neuroethol. Sensory, Neural, Behav. Physiol.* **201**, 5–18 (2015).

32. Römer, H. Directional hearing in insects: biophysical, physiological and ecological challenges. *J. Exp. Biol.* **223**, Pt 14 (2020).

33. Montealegre-Z, F. & Postles, M. Resonant sound production in *Copiphora gorgonensis* (Tettigoniidae: Copiphorini), an endemic species from Parque Nacional Natural Gorgona, Colombia. *J. Orthoptera Res.* **19**, 347–355 (2010).

34. Rossing, T. D. & Fletcher, N. H. *Principles of Vibration and Sound*. (Springer New York, 2004). doi:10.1007/978-1-4757-3822-3.

35. Celiker, E., Jonsson, T. & Montealegre-Z, F. On the tympanic membrane impedance of the katydid *Copiphora gorgonensis* (Insecta: Orthoptera: Tettigoniidae) . *J. Acoust. Soc. Am.* **148**, 1952–1960 (2020).

36. Hummel, J., Wolf, K., Kössl, M. & Nowotny, M. Processing of simple and complex acoustic signals in a tonotopically organized ear. *Proc. R. Soc. B Biol. Sci.* **281**, 20141872 (2014).

37. Windmill, J. F. C., Fullard, J. H. & Robert, D. Mechanics of a `simple' ear: tympanal vibrations in noctuid moths. *J. Exp. Biol.* **210**, 2637–2648 (2007).

38. Bialek, W. Physical limits to sensation and perception. *Annu. Rev. Biophys. Biophys. Chem.* **16**, 455–478 (1987).

39. Windmill, J. F. C., Jackson, J. C., Tuck, E. J. & Robert, D. Keeping up with bats: dynamic auditory tuning in a moth. *Curr. Biol.* **16**, 2418–2423 (2006).

40. Fullard, J. H. External auditory structures in two species of neotropical notodontid moths. *J. Comp. Physiol. A* **155**, 625–632 (1984).

41. Heinrich, R., Jatho, M. & Kalmring, K. Acoustic transmission characteristics of the tympanal tracheae of bushcrickets (Tettigoniidae). II: Comparative studies of the tracheae of seven species. *J. Acoust. Soc. Am.* **93**, 3481–3489 (1993).

42. Bailey, W. J., Stephen, R. O. & Yeoh, P. Signal transmission in noisy environments: Auditory masking in the tympanic nerve of the bushcricket *Metaballus litus* (Orthoptera: Tettigoniinae). *J. Acoust. Soc. Am.* **83**, 1828–1832 (1988).

43. Kalmring, K. & Jatho, M. The effect of blocking inputs of the acoustic trachea on the frequency tuning of primary auditory receptors in two species of tettigoniids. *J. Exp. Zool.* **270**, 360–371 (1994).

44. Bailey, W. J. Do large bushcrickets have more sensitive ears? Natural variation in hearing thresholds within populations of the bushcricket *Requena verticalis* (Listroscelidinae: Tettigoniidae). *Physiol. Entomol.* **23**, 105–112 (1998).

45. Klowden, M. J. CHAPTER 9 - Respiratory Systems. in (ed. Klowden, M. J. B. T.-P. S. in I. (Second E.) 433–461 (Academic Press, 2008). doi:https://doi.org/10.1016/B978-012369493-5.50010-9.

46. Celiker, E., Jonsson, T. & Montealegre-Z, F. The auditory mechanics of the outer ear of the bush cricket: a numerical approach. *Biophys. J.* **118**, 464–475 (2020).

47. Morse, P. & Ingard, K. *Theoretical Acoustics, International Series in Pure and Applied Physics. , Princeton. 412 – 422. Princeton University Press* vol. 170 (1968).

48. Fullard, J. H. Acoustic relationships between tympanate moths and the Hawaiian hoary bat (Lasiurus cinereus semotus). *J. Comp. Physiol. A* **155**, 795–801 (1984).

49. Bailey, W. J. The tettigoniid (Orthoptera□: Tettigoniidae) ear: Multiple functions and structural diversity. *Int. J. Insect Morphol. Embryol.* **22**, 185–205 (1993).

50. Sarria-S, F. A., Chivers, B. D., Soulsbury, C. D. & Montealegre-Z, F. Non-invasive biophysical measurement of travelling waves in the insect inner ear. *R. Soc. Open Sci.* **4**, 1–11 (2017).

51. Rajaraman, K. *et al*. Low-pass filters and differential tympanal tuning in a paleotropical bushcricket with an unusually low frequency call. *J. Exp. Biol.* **216**, 777–787 (2013).

52. Knudsen, E. I. & Konishi, M. Journal of Comparative Physiology-A Mechanisms of Sound Localization in the Barn Owl (*Tyto alba*). *Physiol* **133**, 13–21 (1979).

53. Faure, P. A. & Hoy, R. R. The sounds of silence: cessation of singing and song pausing are ultrasound-induced acoustic startle behaviors in the katydid *Neoconocephalus ensiger* (Orthoptera; Tettigoniidae). *J. Comp. Physiol. A* **186**, 129–142 (2000).

54. Murillo G, O. E., Bedoya, M. J., Velandia-Perilla, J. H. & Yusti-Muñoz, A. P. Riqueza de especies, nuevos registros y actualización del listado taxonómico de la comunidad de murciélagos del Parque Nacional Natural Gorgona, Colombia . *Revista de Biología Tropical* vol. 62 407–417 (2014).

55. Belwood, J. J. & Morris, G. K. Bat predation and its influence on calling behavior in

neotropical katydids. *Science*. **238**, 64–67 (1987).

56. Belwood, J. J. Anti-Predator Defences and Ecology of Neotropical Forest Katydids, Especially the Pseudophyllinae. in *The Tettigoniidae. Biology, systematics and evolution* (eds. Bailey, W. J. & Rentz, D.) 8–26 (Springer-Verlag, 1990).

57. Nickle, D. A. & Castner, J. L. Strategies Utilized by Katydids (Orthoptera: Tettigoniidae) against diurnal predators in rainforests of northeastern Peru. *J. Orthoptera Res*. **4**, 75 (1995).

58. ter Hofstede, H., Kalko, E. K. V & Fullard, J. H. Auditory-based defence against gleaning bats in neotropical katydids (Orthoptera: Tettigoniidae). *J. Comp. Physiol. A. Neuroethol. Sens. Neural. Behav. Physiol.* **196**, 349–358 (2010).

59. ter Hofstede, H. *et al*. Revisiting adaptations of neotropical katydids (Orthoptera: Tettigoniidae) to gleaning bat predation. *Neotrop. Biodivers.* **3**, 41–49 (2017).

60. Montealegre-Z, F., Sarria, F. A., Pimienta, M. C. & Mason, A. C. Lack of correlation between vertical distribution and carrier frequency, and preference for open spaces in arboreal katydids that use extreme ultrasound, in Gorgona, Colombia (Orthoptera: Tettigoniidae). *Rev. Biol. Trop.* **62**, 289 (2014).

61. Kapoor, R., Ramasamy, S., Gardi, A., Van Schyndel, R. & Sabatini, R. Acoustic sensors for air and surface navigation applications. *Sensors (Switzerland)* **18**, (2018).

62. Römer, H. Environmental and biological constraints for the evolution of long-range signalling and hearing in acoustic insects. *Philos. Trans. R. Soc. London. Ser. B Biol. Sci.* **340**, 179–185 (1993).

63. Rentz, D. C. Two new katydids of the genus Melanonotus (*Melanonotus powellorum*) from Costa Rica with comments on their life history strategies (Tettigoniidae:

Pseudophyllinae). *Entomol. News* (1975).

64. Morris, G. K. & Beier, M. Song Structure and Description of Some Costa Rican Katydids (Orthoptera□: Tettigoniidae) Author (s): Glenn K . Morris and Max Beier Source□: Transactions of the American Entomological Society (1890-) , Mar . - Jun ., 1982 , Published by□: American E. **108**, 287–314 (1982).

65. Morris, G. K., Mason, A. C., Wall, P. & Belwood, J. J. High ultrasonic and tremulation signals in neotropical katydids (Orthoptera: Tettigoniidae). *J. Zool.* **233**, 129–163 (1994).

66. Heller, K. G. Acoustic signalling in palaeotropical bushcrickets (Orthoptera: Tettigonioidea: Pseudophyllidae): does predation pressure by eavesdropping enemies differ in the Palaeo□ and Neotropics? *J. Zool.* **237**, 469–485 (1995).

67. Geipel, I. *et al.* Bats actively use leaves as specular reflectors to detect acoustically camouflaged prey. *Curr. Biol.* **29**, 2731-2736.e3 (2019).

68. Geipel, I. *et al.* Predation risks of signalling and searching: Bats prefer moving katydids. *Biol. Lett.* **16**, 3–7 (2020).

69. Robinson, D. J. & Hall, M. J. Sound signalling in orthoptera. *Adv. In Insect Phys.* **29**, 151–278 (2002).

70. Page, R. & Bernal, X. E. The challenge of detecting prey: Private and social information use in predatory bats. *Funct. Ecol.* **34**, 344–363 (2020).

71. Falk, J. J. *et al.* Sensory-based niche partitioning in a multiple predator-multiple prey community. *Proc. R. Soc. B Biol. Sci.* **282**, (2015).

72. Geipel, I., Lattenkamp, E. Z., Dixon, M. M., Wiegrebe, L. & Page, R. A. Hearing sensitivity: An underlying mechanism for niche differentiation in gleaning bats. *Proc.*

Natl. Acad. Sci. U. S. A. **118**, (2021).

73. Geipel, I., Jung, K. & Kalko, E. K. V. Perception of silent and motionless prey on vegetation by echolocation in the gleaning bat *Micronycteris microtis*. *Proc. R. Soc. B Biol. Sci.* **280**, (2013).

74. Yoh, N., Syme, P., Rocha, R., Meyer, C. F. J. & López-Baucells, A. Echolocation of Central Amazonian 'whispering' phyllostomid bats: call design and interspecific variation. *Mammal Res.* **65**, 583–597 (2020).

75. Plotnick, R. O. Y. E. & Smith, D. M. Exceptionally preserved fossil insect ears from the Eocene Green River formation of Colorado. *J. Paleontol.* **86**, 19–24 (2012).

76. Greenwalt, D. E. & Rust, J. E. S. A new species of *Pseudotettigonia Zeuner* (Orthoptera: Tettigoniidae) with an intact stridulatory field and reexamination of the subfamily Pseudotettigoniinae. *Syst. Entomol.* **39**, 256–263 (2014).

77. Rust, J., Stumpner, A. & Gottwald, J. Singing and hearing in a Tertiary bushcricket. *Nature* **399**, 650 (1999).

78. Teeling, E. C. *et al.* A molecular phylogeny for bats illuminates biogeography and the fossil record. *Science.* **307**, 580 LP – 584 (2005).

79. Mugleston, J. D., Song, H. & Whiting, M. F. A century of paraphyly: a molecular phylogeny of katydids (Orthoptera: Tettigoniidae) supports multiple origins of leaf-like wings. *Mol. Phylogenet. Evol.* **69**, 1120–1134 (2013).

80. Vicente, N. *et al.* In and out of the Neotropics: historical biogeography of Eneopterinae crickets. *J. Biogeogr.* **44**, 2199–2210 (2017).

81. Schneider, E. S., Römer, H., Robillard, T. & Schmidt, A. K. D. Hearing with exceptionally thin tympana: Ear morphology and tympanal membrane vibrations in

eneopterine crickets. *Sci. Rep.* **7**, 1–12 (2017).

82. Lang, A. B. & Römer, H. Roost site selection and site fidelity in the neotropical katydid *Docidocercus gigliotosi* (Tettigoniidae). *Biotropica* **40**, 183–189 (2008).

83. Fornoff, F., Dechmann, D. K. N. & Wikelski, M. Observation of movement and activity via radio-telemetry reveals diurnal behavior of the neotropical katydid *Philophyllia ingens* (Orthoptera: Tettigoniidae). *Ecotropica* **18**, 27–34 (2012).

84. COMSOL Multiphysics.

85. Courant, R., Friedrichs, K. & Lewy, H. On the Partial Difference Equations of Mathematical Physics. *IBM J. Res. Dev.* **11**, 215–234 (1967).

86. Lenth, R. & Lenth, M. R. Package 'lsmeans'. *Am. Stat.* **34**, 216–221 (2018).

87. Kuznetsova, A., Brockhoff, P. B. & Christensen, R. H. B. lmerTest Package: Tests in Linear Mixed Effects Models. *J. Stat. Software; Vol 1, Issue 13* (2017).

88. Team, R. C. R: A language and environment for statistical computing. (2021).

Figure legends

Figure 1. A. Location of the ear in the foreleg, external auditory input of *Copiphora gorgonensis*. **B.** 3D anatomy of the ear, with pinnae present; **C**. 3D anatomy of the following pinnae ablation, with the volume of the subslit cavities exhibited (light blue); **D**. 3D model of only the subslit cavities.

Figure 2. A. Time plots from five incidence angles for the 60 kHz test sound illustrating changes in oscillation phase between the anterior (ATM) and posterior (PTM) tympana of the same ear. An anatomical cross section of the ear is shown with each tympanum (ATM and

PTM), auditory vesicle (AV), posterior and anterior bifurcated tracheal branches (PT and AT), haemolymph channel (HC) and posterior and anterior pinnal structures (PP and AP). **B**. Mean displacement amplitudes (nm) of the tympanic membranes for each tested frequency (23, 40 and 60 kHz) with and without the presence of cuticular pinnae (*n* = 9 ears; df = 1711). **C**. Mean arrival times (ms) of presented stimuli of 23, 40 and 60 kHz with and without the pinnae from time domain recordings of live experimental specimens (*n* = 9 ears; df = 1711). **D**. Cavity induced pressure gains (with pinnae) compared to sound pressure (dB) predictions with the pinnae ablated from mathematical numerical models (17 ears; 10 females, 7 males). **E**. Simulated arrival times (ms) of selected frequencies (23, 40 and 60 kHz) using Comsol Multiphysics, v.5.6 (17 ears; 10 females, 7 males). For means comparison plots (**B** – **E**), significance symbols: '***' 0.001 '**' 0.01 '*' 0.05 'ns' 0.1 ' ' 1. Red bars with cuticular pinnae and blue bars without cuticular pinnae.

Figure 3. Panels **A**, **C**, and **E** depict cavity induced sound pressure distribution and gains with pinnae, panels **B**, **D**, and **F** represent sound pressure gains without the pinnae. **A** and **B**. Cross – section of the ear of *Copiphora gorgonensis* with the pinnal structures intact (**A**) and ablated (**B**). Sound pressure intensities depicted with colours for simulations of 23, 40, 60 and 110 kHz. Low sound pressure dB (blue) to high sound pressure dB (red) distributions inside and outside the cavities. **C** and **D** are plots of simulated sound pressure gains (dB SPL) in the frequency ranges of 20 – 150 kHz for each tympanum. **E** and **F** are plots of relative dB gain of the tympanal cavities in the 3D printed ears. ATM in red bars and PTM in blue bars.

Figure 4. A. Sound pressure gains (dB SPL) of 3D printed ears calculated from scaled time

domain recordings for 23, 40, 60 and 110 kHz. Photos of 3D printed ear models with pinnae present (**B**) and ablated (**C**) and probe microphone placement.

Figure 5. Ecological relevance of pinnae in *Copiphora gorgonensis*. Sound pressure level gains (left) induced by the pinnae are present only at frequencies above c.a. 60 kHz, covering the range of echolocation frequencies of five native insectivorous gleaning bat species. The conspecific call of *C. gorgonensis* on the other hand (dB_{peak} at 23 kHz), is not enhanced by the presence of the pinnae (dB loss). Dotted line indicates the frequency at which gain = 0 dB. Spectrogram parameters: FFT size 512, Hamming window, 50% overlap; frequency resolution: 512 Hz, temporal resolution: 0.078 ms.

Figures

Figure 1

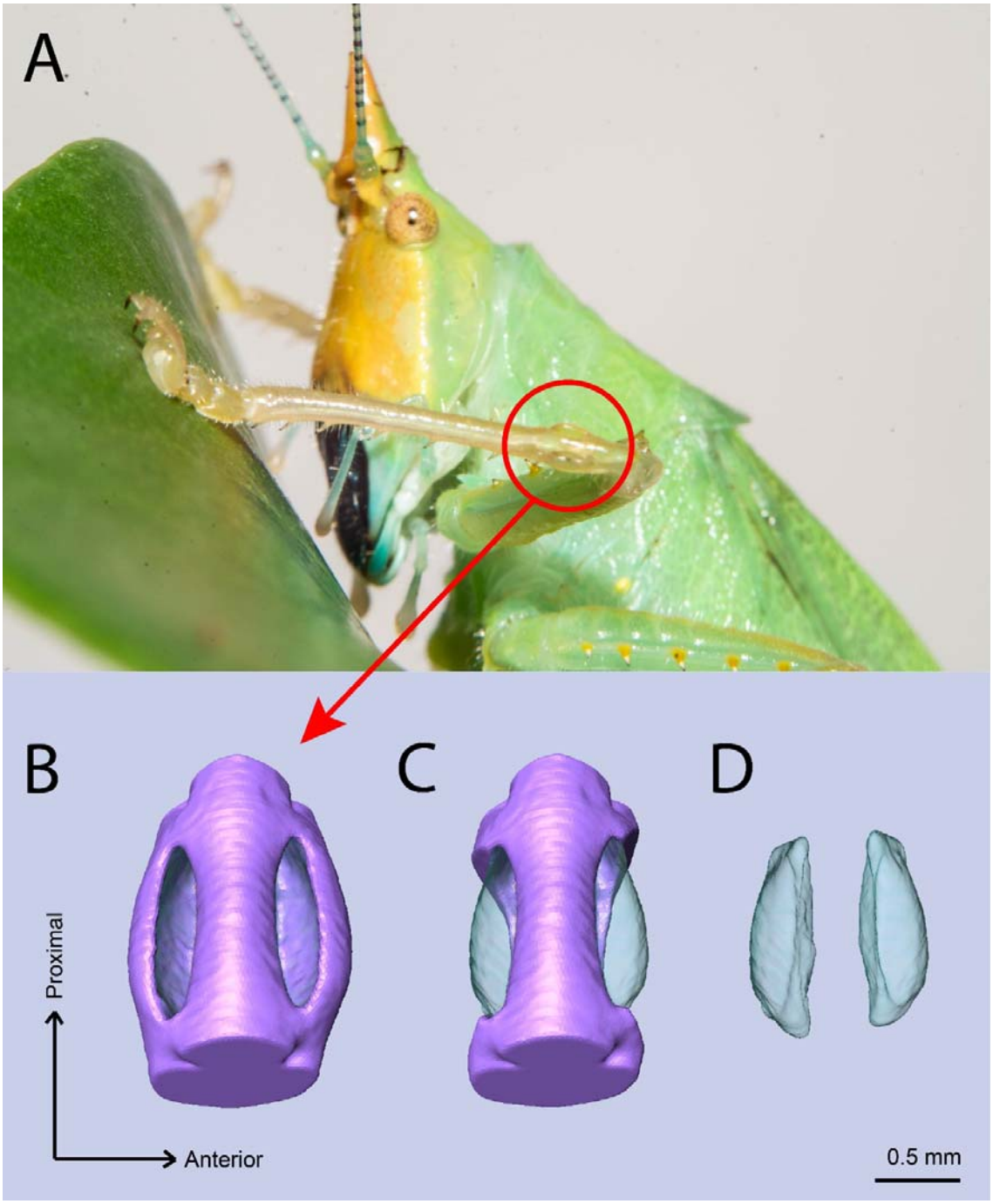

Figure 2

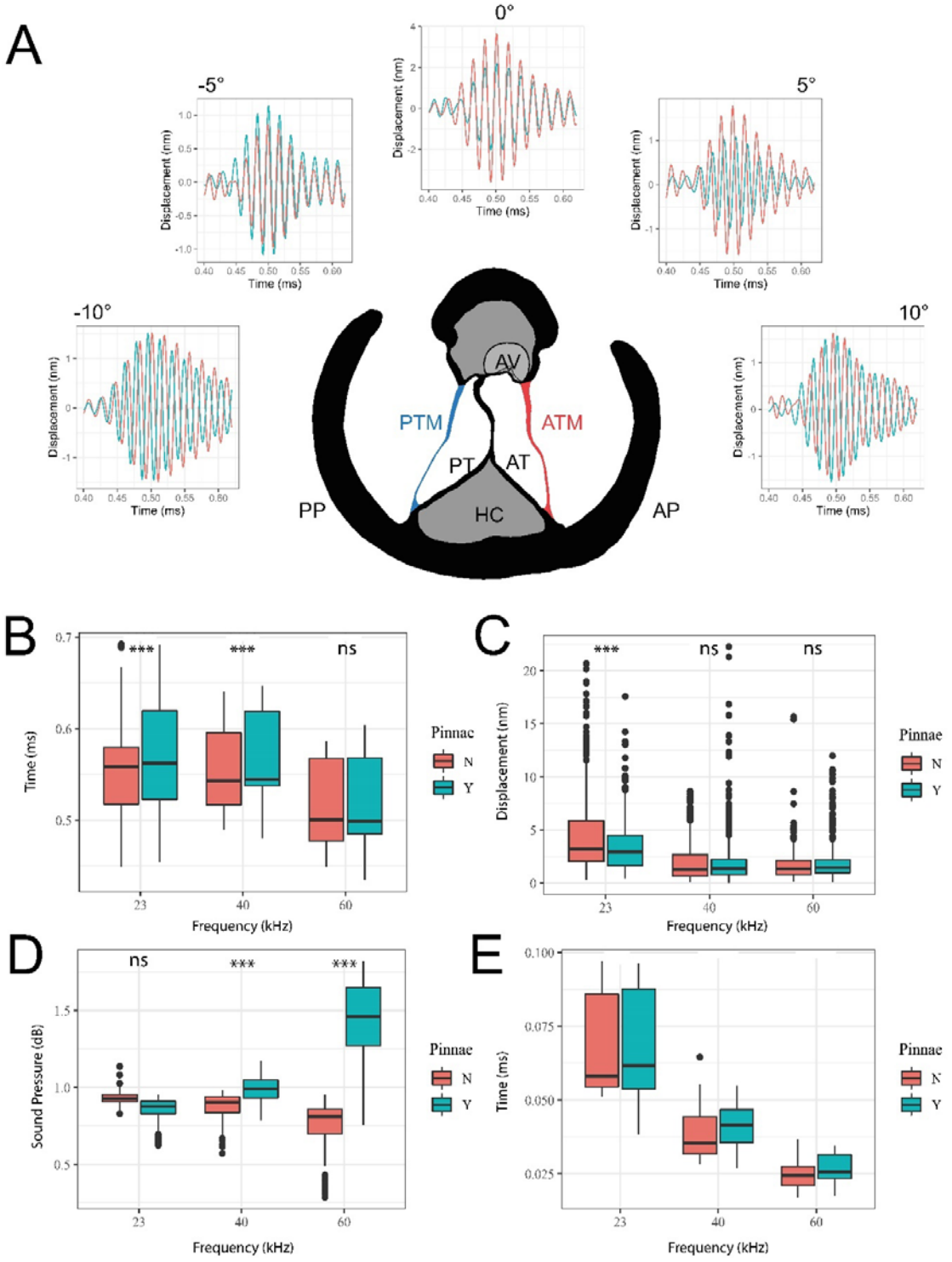
A
-5°
0°
5°
-10°
10°
Displacement (nm)
Time (ms)
AV
PTM
ATM
PT
AT
HC
PP
AP
B
C
D
E
***
ns
Time (ms)
Displacement (nm)
Sound Pressure (dB)
Frequency (kHz)
Pinnae
N
Y

Figure 3

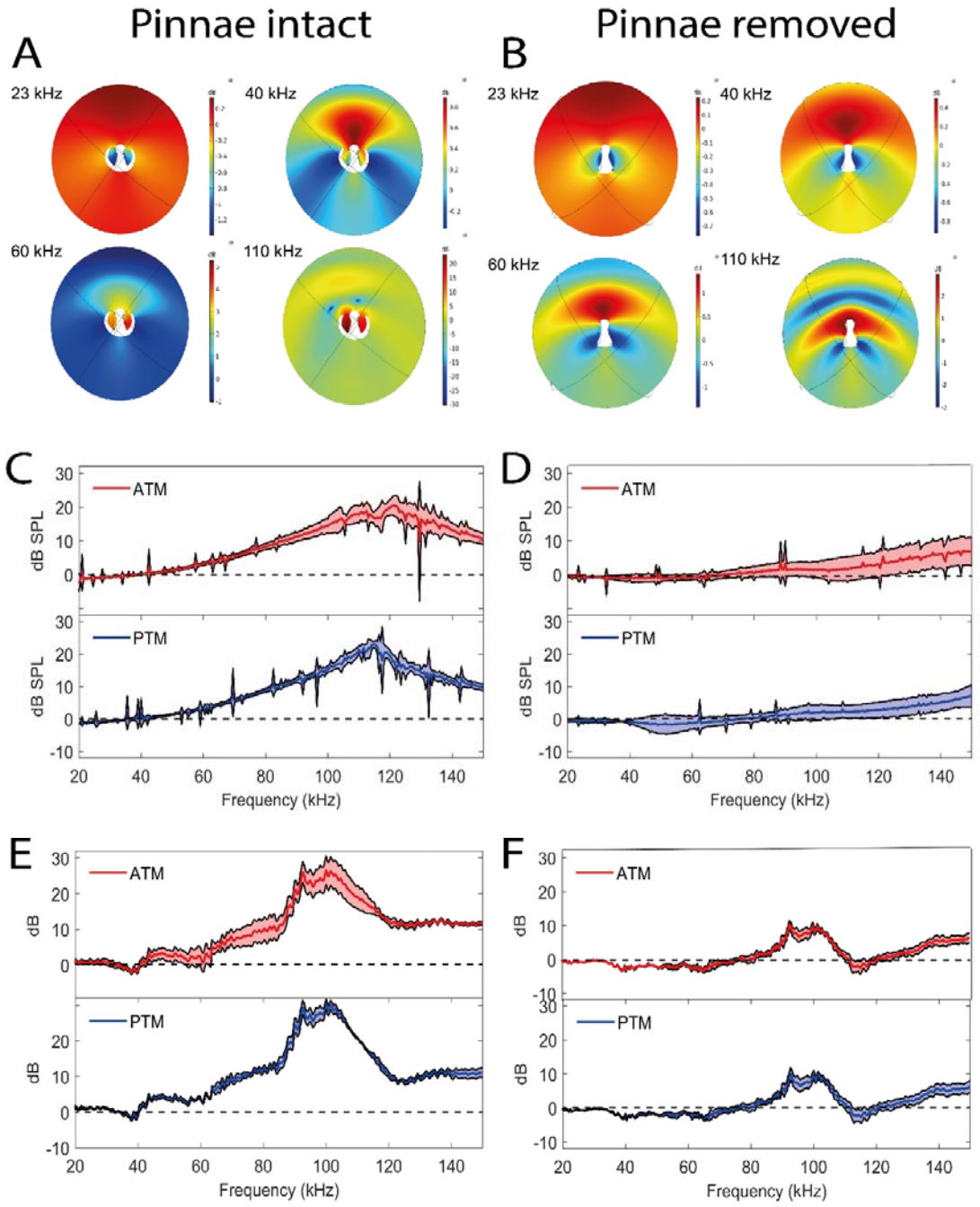
Pinnae intact
Pinnae removed
A
B
23 kHz
40 kHz
60 kHz
110 kHz
C
D
E
F
ATM
PTM
dB SPL
dB
Frequency (kHz)

Figure 4

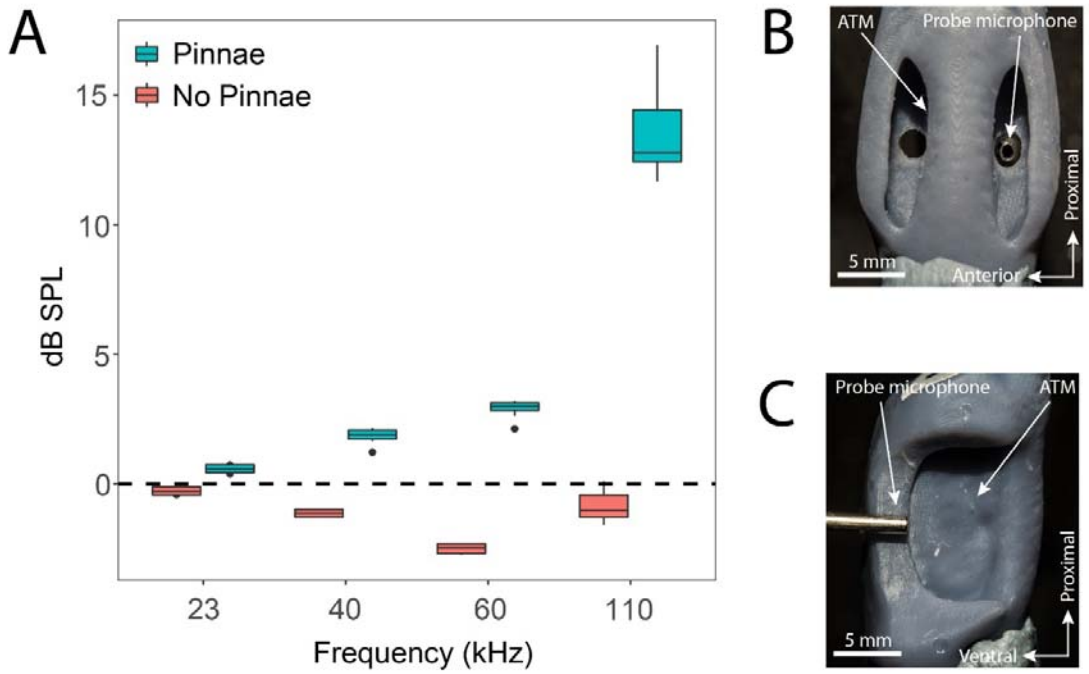
A
Pinnae
No Pinnae
15
10
5
0
dB SPL
23
40
60
110
Frequency (kHz)
B
ATM
Probe microphone
Proximal
5 mm
Anterior
C
Probe microphone
ATM
Proximal
5 mm
Ventral

Figure 5

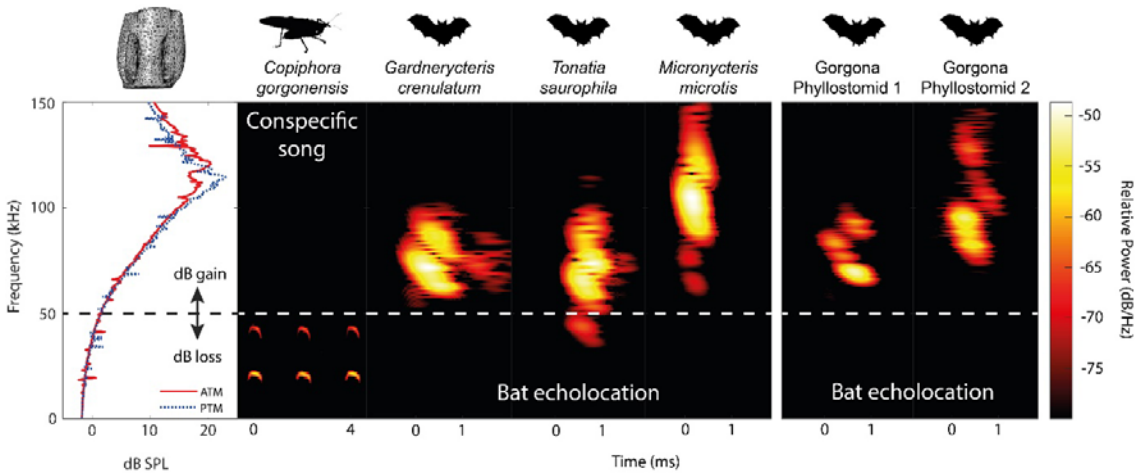
Copiphora gorgonensis
Gardnerycteris crenulatum
Tonatia saurophila
Micronycteris microtis
Gorgona Phyllostomid 1
Gorgona Phyllostomid 2
Conspecific song
Bat echolocation
Bat echolocation
Frequency (kHz)
dB gain
dB loss
ATM
PTM
dB SPL
Time (ms)
Relative Power (dB/Hz)